Paper 229

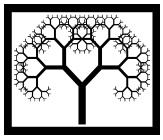

Proceedings of the Eleventh International Conference on Computational Structures Technology,
B.H.V. Topping, (Editor),
Civil-Comp Press, Stirlingshire, Scotland

Estimation of Critical Flutter Load of a Non-Uniform L-Shaped Beam subjected to a Follower Force

I. Takahashi
Department of Mechanical Engineering
Kanagawa Institute of Technology, Japan

Abstract

With increasing size and complexity of machines and vessels, the inverse problems of continuous bodies are becoming important. In this paper the possibility of using a response surface methodology, which consists of a design of experiments, for estimating the critical flutter load of the tapered L-shaped beam is studied. An analysis is presented for the vibration and stability of a non-uniform beam subjected to tangential follower forces distributed over the center line by use of the transfer matrix approach.

Keywords: Response surface approximation, design of experiments, vibration, L-shaped beam, critical flutter load.

1 Introduction

Light weight structure have been extensively used in many industrial fields such as in mechanical, aerospace and rocket engineering, and therefore vibration and stability problems of beams have become of increasing importance. There is a considerable number of papers available on the non-conservative instability of Bernouli-Euler beams subjected to follower force.

Bolotin has extensively studied the non-conservative problems of elastic stability, detailed explanations for which are provided in his book [1]. Kounadis and Katsikadelis [2] studied the flutter loads of Beck's columns with the shear deformation and rotatory inertia taken into account. Saito and Otomi [3] have studied the vibration and stability of beams with an attached mass under axial and tangential loads. Irie *et al* . [4] calculated the critical flutter loads of a Timoshenko beam of a cross-section prescribed by an arbitrary function subjected to a follower force of various types. On the other hand, many researchers (see e.g. Venkateswara and Kanaka [5], Lee, *et al.* [6], Lee and Yang [7]) have analyzed the non-conservative

instability of beams resting on an elastic foundation. De Rosa and Franciosi [8], and Takahashi and Yoshioka [9] have studied the influence of an intermediate support on the stability behavior of cantilever beams and double beams subjected to follower forces. Singh, *et al*. [10] discussed the implementation of follower and axial end forces in beam-type MEMS resonator for the application of resonant frequency tuning. Furthermore, Takahashi and Yoshioka [11] have studied the stability behavior and in-plane vibration of L-shaped cantilever beams subjected to follower forces. Takahashi [12] have studied the identification method for the critical force of a non-uniform L-shaped cracked shaft using the neural networks.

The problem of experimental design or design of experiments (DOE) is encountered in many fields. A common situation for using DOE is when the designer does not know the exact underlying relationship between responses and design variables. The empirical model is called a response surface model or curve fit. The basic idea of response surface methodology is to create explicit approximation functions to the objective and constraints, and then use these when performing the optimization. The approximation functions are typically in the form of low-order polynominals fit by least squares regression analysis. In order to construct the approximation function, it is necessary to have some results for a minimum number of points in the design space. The proper selection of points could drastically improve the quality of a response surface model. The response at the most suitable points, which are selected by the design of experiments (DOE) could have been obtained either by some analysis program or through physical experiments.

In this paper the possibility of using a resopnse surface methodology, which consists of a design of experiments, for estimating the critical flutter load of the L-shaped beam is studied. An analysis is presented for the out-of-plane vibration and stability of a tapered beam subjected to a follower force by use of the transfer matrix approach. Once the matrix has been determined by the numerical integration of equations, the eigenvalues of vibration and the critical flutter load are obtained. The method is applied to beams with linearly varying cross-sections, and the natural frequencies and flutter loads are calculated numerically, to provide information about the effect on them of varying cross-section, span and stiffness of intermediate supports, opening angle and slenderness ratio.

2 Application to Non-uniform Beam

2.1 Analysis of Non-Uniform L-shaped Beam and Data

An L-shaped beam with a circular cross-section is shown in Figure 1. We consider a non-uniform Timoshenko beam of length *l,* part C of which is subjected to a tangential follower force. The origin *o* is taken at one end of the beam, and the shear center axis is taken as the *x*-axis. With the rotatory inertia and shear deformation taken into account, the equations of flexural motion of the beam (for part C) when subjected to a tangential follower force *f(s)* , which is distributed over the axis can be written as (see e.g. [12])

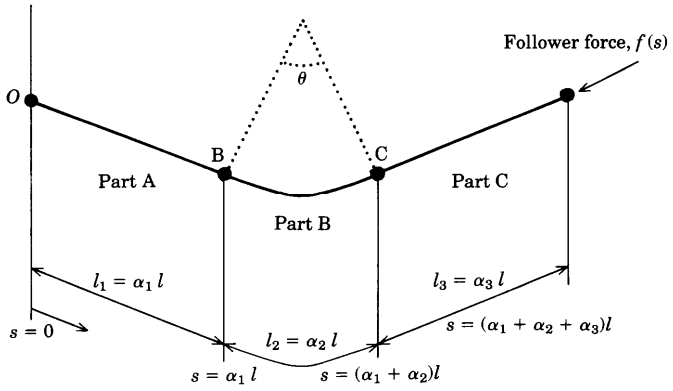

Figure 1. A non-uniform L-shaped beam subjected to a follower force

$$\frac{dQ^*}{ds} - f(s)\frac{d^2w^*}{ds^2} + \rho A(s)\omega^2 w^* = 0 \tag{1}$$

$$Q^* - \frac{dM^*}{ds} + \rho I(s)\omega^2 \psi^* = 0 \tag{2}$$

where ρ is the mass per unit volume, $A(s)$ is the cross-sectional area, and $I(s)$ is the second moment of area of the beam. The variables w^* and ψ^* denote the transverse deflection and the slope due to pure bending, respectively. The variable ω is the natural frequency. The bending moment M^* and shear force Q^*, respectively, are given by

$$M^* = -EI_x(s)\frac{d\psi^*}{ds} \tag{3}$$

$$Q^* = \{\kappa GA(s) + f(s)\}\left(\frac{dw^*}{ds} - \psi^*\right) \tag{4}$$

where E is Young's modulus and G is the shear modulus.

Also, the equations of torsional motion of the beam are written as

$$\frac{dT^*}{ds} + \rho I_p(s)\omega^2\theta^* = 0 \tag{5}$$

$$T^* = GI_p(s)\frac{d\theta^*}{ds} \tag{6}$$

where θ^* is the total angle of twist and T^* is the torque. For part A, the follower force $f(s)$ in Equations (1) and (4) is zero.

With the length measured along the neutral axis of the beam of radius $\overline{R}$ denoted by s , and the opening angle by θ_1 , the $x-$ and $z-$azes are taken in the radial and tangential directions, respectively. The equations of out-of-plane vibration of the beam (for part B) are written as

$$\frac{d\overline{Q_y^*}}{ds} + \rho A(s)\omega^2 \overline{v^*} = 0 \tag{7}$$

$$\frac{d\overline{M_x^*}}{ds} + \frac{\overline{T^*}}{\overline{R}} - \overline{Q_y^*} + \rho I_x(s)\omega^2 \overline{\phi^*} = 0 \tag{8}$$

$$\frac{d\overline{T}}{ds} - \frac{\overline{M_x^*}}{\overline{R}} + \rho I_p(s)\omega^2 \overline{\psi^*} = 0 \tag{9}$$

where $I_x(s), I_p(s)$ are the second moment and polar moment of area, respectively.

The shearing force $\overline{Q_y^*}$, bending moment $\overline{M_x^*}$ and torsional moment $\overline{T^*}$, respectively, are given by

$$\overline{Q_y^*} = kGA(s)\left(\overline{\phi^*} + \frac{d\overline{v^*}}{ds}\right) \tag{10}$$

$$\overline{M_x^*} = \frac{EI_x(s)}{\overline{R}}\left(\overline{\psi^*} + \overline{R}\frac{d\overline{\phi^*}}{ds}\right) \tag{11}$$

$$\overline{T^*} = \frac{GC_z(s)}{\overline{R}}\left(-\overline{\phi^*} + \overline{R}\frac{d\overline{\psi}}{ds}\right) \tag{12}$$

in terms of the transverse deflection $\overline{v^*}$, the slope $\overline{\phi^*}$ due to pure bending and angle of the torsion $\overline{\psi^*}$. The quantity C_Z is the St. Venant torsional constant of the cross-section.

For simplicity of the analysis, the following dimensionless variables are introduced:

$$w^* = wl \qquad \overline{v^*} = vl$$

$$\psi^* = \psi \qquad \overline{\phi^*} = \overline{\phi}$$

$$\theta^* = \theta \qquad \overline{\psi^*} = \overline{\psi}$$

$$Q^* = \frac{EI_{x0}}{l^2}Q \qquad \overline{Q_y^*} = \frac{EI_{x0}}{l^2}\overline{Q_y}$$

$$M^* = \frac{EI_{x0}}{l}M \qquad \overline{M_x^*} = \frac{EI_{x0}}{l}\overline{M_x}$$

$$T^* = \frac{EI_{x0}}{l}T \qquad \overline{T^*} = \frac{EI_{x0}}{l}\overline{T}$$

$$\eta = \frac{s}{l} \ , \ a = \frac{A(s)}{A_0} \ , \ i_x = \frac{I_x(s)}{I_{x0}} \ , \ i_p = \frac{I_p(s)}{I_{p0}}, \quad r = \frac{\overline{R}}{l}$$

$$s_{x0}^2 = \frac{A_0 l^2}{I_{x0}} \ , \ s_{y0}^2 = \frac{A_0 l^2}{I_{y0}} \ , \ k_z = \frac{C_z(s)}{C_{z0}} \ , \ \mu = \frac{GC_{z0}}{EI_{x0}} = \frac{GI_{p0}}{EI_{x0}} \ ,$$

$$p = \frac{l^2}{EI_{x0}} f(s)$$

$$g_e = \frac{G}{E}, \quad \tilde{A} = \kappa \, g_e s_{x0}^2, \quad \tilde{g} = \tilde{A} \, a + p \tag{13}$$

Here A_0 and I_{x0} are the sectional area and the second moment of area at one end ($s = 0$). The value s_{x0}, s_{y0} are the slenderness ratios at one end. The quantities without an asterisk (*) are the respective dimensionless variables. As a frequency parameter

$$\lambda^4 = \frac{\rho A_0 l^4 \omega^2}{EI_{x0}} \tag{14}$$

is used here.

Equations (7)-(12) for the beam are written as a matrix differential equation

$$\frac{d}{d\eta}\{Z(\eta)\} = [U(\eta)] \ \{Z(\eta)\} \tag{15}$$

where the state vector $\{Z(\eta)\} = \{w \quad \psi \quad \theta \quad Q \quad M \quad T\}^T$ and the coefficient matrix $[U(\eta)]$.

$$U_{12} = 1, \quad U_{14} = \frac{1}{\tilde{g}}, \quad U_{11} = U_{13} = U_{15} = U_{16} = 0$$

$$U_{25} = -\frac{1}{i_x}, \quad U_{21} = U_{22} = U_{23} = U_{24} = U_{26} = 0$$

$$U_{36} = \frac{1}{i_p \mu}, \quad U_{31} = U_{32} = U_{33} = U_{34} = U_{35} = 0$$

$$U_{41} = -\frac{\lambda^4 a}{\left(1 - \frac{p}{\tilde{g}}\right)}, \quad U_{44} = -\frac{p}{\left(1 - \frac{p}{\tilde{g}}\right)} \frac{\tilde{g}'}{\tilde{g}^2}, \quad U_{45} = -\frac{p}{\left(1 - \frac{p}{\tilde{g}}\right)} \frac{1}{i_x}, \quad U_{42} = U_{43} = U_{46} = 0$$

$$U_{52}=\frac{\lambda^4 i_x}{s_{x0}^2},\quad U_{54}=1,\quad U_{51}=U_{53}=U_{55}=U_{56}=0$$

$$U_{63}=-\frac{\lambda^4}{s_{x0}^2}\frac{\mu}{g_e}i_p,\qquad U_{61}=U_{62}=U_{64}=U_{65}=U_{66}=0 \tag{16}$$

Equations (7)-(12) for the circular beam are written as a matrix differential equation

$$\frac{d}{d\eta}\left\{\overline{Z}(\eta)\right\}=\left[\overline{U}(\eta)\right]\ \left\{\overline{Z}(\eta)\right\} \tag{17}$$

where the state vector $\{\overline{Z}(\eta)\}=\{\overline{v}\quad\overline{\phi}\quad\overline{\psi}\quad\overline{Q_y}\quad\overline{M_x}\quad\overline{T}\}^T$ and the coefficient matrix $[\overline{U}(\eta)]$.

$$\bar{U}_{12}=-1,\quad \bar{U}_{14}=\frac{1}{\tilde{A}\,a},\qquad \bar{U}_{11}=\bar{U}_{13}=\bar{U}_{15}=\bar{U}_{16}=0$$

$$\bar{U}_{23}=-\frac{1}{r},\quad \bar{U}_{25}=\frac{1}{i_x},\quad \bar{U}_{21}=\bar{U}_{22}=\bar{U}_{24}=\bar{U}_{26}=0$$

$$\bar{U}_{32}=\frac{1}{r},\quad \bar{U}_{36}=\frac{1}{k_z\mu},\qquad \bar{U}_{31}=\bar{U}_{33}=\bar{U}_{34}=\bar{U}_{35}=0$$

$$\bar{U}_{41}=-\lambda^4 a\ ,\qquad \bar{U}_{42}=\bar{U}_{43}=\bar{U}_{44}=\bar{U}_{45}=\bar{U}_{46}=0$$

$$\bar{U}_{52}=-\frac{\lambda^4}{s_{x0}^2}i_x,\quad \bar{U}_{54}=1,\quad \bar{U}_{56}=-\frac{1}{r},\qquad \bar{U}_{51}=\bar{U}_{53}=\bar{U}_{55}=0$$

$$\bar{U}_{63}=-\frac{\lambda^4}{s_{x0}^2}\frac{\mu}{g_e}i_p,\quad \bar{U}_{65}=\frac{1}{r},\qquad \bar{U}_{61}=\bar{U}_{62}=\bar{U}_{64}=\bar{U}_{66}=0 \tag{18}$$

Since analytical solutions of Equations (15) and (17) cannot be obtained for a beam with varying cross-section, the transfer matrix approach is adopted here. In general, the state vector $\{Z(\eta)\}$ can be expressed as

$$\left\{Z(\eta)\right\}=\left[T(\eta)\right]\ \left\{Z(0)\right\} \tag{19}$$

by using the transfer matrix $[T(\eta)]$ of the beam. From Equations (15) and (19), the following equation is derived:

$$\frac{d}{d\eta}\left[T(\eta)\right]=\left[U(\eta)\right]\ \left[T(\eta)\right] \tag{20}$$

For a beam of varying cross-section, the matrix $[T(\eta)]$ is obtained by integrating Equation (20) numerically with the starting value $[T(0)]=[I]$(the unit matrix), which is given by taking $\eta=0$ in Equation (19). In the calculation, the elements of the transfer

matrix are determined numerically by using Runge-Kutta integration method. The solution of Euqation (17) is also obtained by the same procedure.

The continuity at the connecting point B yields

$$\left\{\overline{Z}(\alpha_1)\right\}_{(R)} = \left[P_B\right]_{(\alpha 1)}\left\{Z(\alpha_1)\right\}_{(L)} \tag{21}$$

by use of the point matrix $[P_B]_{(\alpha 1)}$.

The continuity at the connecting point C is similarly expressed as

$$\left\{Z(\alpha_1+\alpha_2)\right\}_{(R)} = \left[P_C\right]_{(\alpha 1+\alpha 2)}\left\{\overline{Z}(\alpha_1+\alpha_2)\right\}_{(L)} \tag{22}$$

The continuity at intermediate supports ($at\ \eta=\beta_i (stiffness:\ \ k_i)$, $i=1,2$) also yields

$$\left\{Z\ (\beta_i)\right\}_{(R)} = \left[P_i\right]\ \left\{Z\ (\beta_i)\right\}_{(L)}\quad (0<\beta_1<\alpha_1)\ \ or\ \ (\alpha_1+\alpha_2<\beta_2<1) \tag{23}$$

Substitution of Equation (19) into Equations (21)-(23) yields

$$\left\{Z(1)\right\} = \left[M\right]_{(1)}\left\{Z(0)\right\} \tag{24}$$

where the final transfer matrix of the beam ($0<\beta_1<\alpha_1<\alpha_1+\alpha_2<\beta_2<1$) is

$$\left[M\right]_{(1)} = \left[T\right]_{(1)}\left[P_2\right]_{(\beta_2)}\left[T\right]_{(\beta_2)}\left[P_C\right]_{(\alpha 1+\alpha 2)}\left[\overline{T}\right]_{(\alpha 1+\alpha 2)}\left[P_B\right]_{(\alpha 1)}\left[T\right]_{(\alpha 1)}\left[P_1\right]_{(\beta_1)}\left[T\right]_{(\beta_1)} \tag{25}$$

This method can be applied to any combination of boundary conditions of the beam. Here, a cantilever beam will be discussed. The boundary conditions are

$$\begin{aligned} &w=0, \quad \psi=0, \quad \theta=0 \quad at \quad \eta=0 \\ &Q=0, \quad M=0, \quad T=0 \quad at \quad \eta=1 \end{aligned} \tag{26}$$

Since $[T(\eta)]$ depend on the frequency parameter λ, $[M]_{(1)}$ is also a function of λ. The natural frequencies of the beam are determined by calculating the eigenvalues λ of Equations (24) and (26).

The numerical calculations were carried out for the free-clamped beams subjected to a concentrated follower force. The beam has the intermediate supports at $\eta=\beta_1$ and $\eta=\beta_2$. The method is applied to L-shaped beams with linearly varying diameter d_1/d_0, and the natural frequencies are calculated numerically, to provide information about the effect on them of varying cross-section, span and stiffness of intermediate supports, opening angle and slenderness ratio.

Figure 2 shows the model eigenvalue curve of a cantilever beam subjected to a concentrated follower force at the free edge. The values (λ_1 - λ_4) of the curve on the ordinate indicate the eigenvalues of the beam without the action of the follower force. With increasing force (p), the eigenvalues of the first mode increase, while those of the second mode decrease. The maximum of the branch of the eigenvalue curve indicates the critical flutter load $p_{B,f}$ beyond which the natural frequencies become complex quantities and therefore, the motion becomes an unstable vibration with exponentially increasing amplitude.

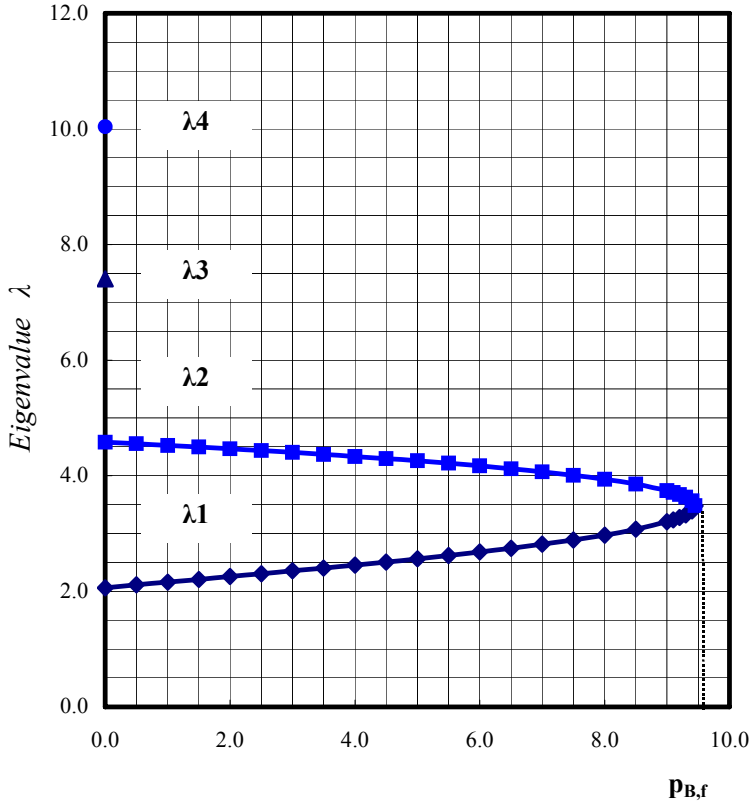

Figure 2. Eigenvalue curve

2.2 Response Surface Approximation

The basic idea of response surface methodology is to create explicit approximation functions to the objective and constraints, and then use these when performing the optimization. The approximation functions are typically in the form of low-order polynominals fit by least squares regression analysis.Once approximations have been constructed, they may be used as cheap function evaluations, replacing the underlying computationally expensive analysis tools. In order to construct the approximation function, it is necessary to have some results for a minimum number of points in the design space. The response at the most suitable points, which are selected by the design of experiments (DOE) could have been obtained either by some analysis program or through physical experiments.

Consider a simple case of a quadratic response model. The typical quadratic polynominals is written as follows.

$$y = \bar{\alpha}_0 + \sum_{j=1}^{k} \bar{\alpha}_j x_j + \sum_{j=1}^{k} \bar{\alpha}_j x_j^2 + \sum_{i=1}^{k-1} \sum_{j=i+1}^{k} \bar{\alpha}_{ij} x_i x_j \qquad (27)$$

where $\bar{\alpha}$ are the regression coefficients and k is total number of the predictor variables. For the case of two variables, Eqation (27) can be written as follows.

$$y = \bar{\alpha}_0 + \bar{\alpha}_1 x_1 + \bar{\alpha}_2 x_2 + \bar{\alpha}_3 x_1^2 + \bar{\alpha}_4 x_2^2 + \bar{\alpha}_5 x_1 x_2 \tag{28}$$

Replacing $x_3 = x_1^2, x_4 = x_2^2, x_5 = x_1 x_2$, Eqation (28) can be transformed to a linear multiple regression.

The true response **y** can be written in the follwong matrix form in terms of n observations.

$$\mathbf{y} = \mathbf{X}\bar{\boldsymbol{\alpha}} + \mathbf{e} \tag{29}$$

Where $\bar{\boldsymbol{\alpha}}, \mathbf{e}$ and $\mathbf{X}$ are the matrix form of regression coefficient, approximation error and predictor variable, respectively.

$$\mathbf{y} = \left(y_1\ y_2\ \ldots y_n\right)^T, \bar{\boldsymbol{\alpha}} = \left(\bar{\alpha}_0 \bar{\alpha}_1\ \ldots \bar{\alpha}_k\right)^T, \mathbf{e} = \left(e_1\ e_2\ \ldots e_n\right)^T$$

$$y = \begin{pmatrix} 1 & x_{11} & \cdots & x_{1k} \\ 1 & x_{21} & \cdots & x_{2k} \\ \vdots & \vdots & \ddots & \vdots \\ 1 & x_{n1} & \cdots & x_{nk} \end{pmatrix} \tag{30}$$

From Eqation (29), The sum of squares of the error terms(SS_E) is given by

$$SS_E = \mathbf{e}^T\mathbf{e} = (\mathbf{y} - \mathbf{X}\bar{\boldsymbol{\alpha}})^T(\mathbf{y} - \mathbf{X}\bar{\boldsymbol{\alpha}}) = \mathbf{y}^T\mathbf{y} - 2\bar{\boldsymbol{\alpha}}^T\mathbf{X}\mathbf{y} - \bar{\boldsymbol{\alpha}}^T\mathbf{X}^T\mathbf{X}\bar{\boldsymbol{\alpha}} \tag{31}$$

To minimize the sum of squares of the error terms, the first derivative of SS_E should be zero

$$\frac{\partial\ (SS_E)}{\partial \bar{\alpha}} = -2\mathbf{X}^T\mathbf{y} + 2\mathbf{X}^T\mathbf{X}\bar{\boldsymbol{\alpha}} = 0 \tag{32}$$

From Eqation (32) the estimate of $\boldsymbol{\alpha}$ that provides us with the minimum sum of squares of error terms is:

$$\mathbf{b} = (\mathbf{X}^T\mathbf{X})^{-1}\mathbf{X}^T\mathbf{y} \tag{33}$$

Eqation (33) is a solution of the least squares problem that is applicable to problems with any number of terms, k, in the response surface model and for any number of design points, n, provided that $n \geq k$.

Response surface method consists of a design of experiments to select the most suitable points for fitting the surfaces effectively. In this paper, the two or three-level orthogonal Latin squares is used. Orthogonal Latin squares are special matrices used as design matrices, $\mathbf{D}$, in fractional factorial design. These Latin squares allow the effects of several parameters to be determined efficiently. For 3-level orthogonal Latin squares, each of the design variables has exactly three levels that are

represented in the columns of the design matrix, **D**. For any pair columns, all combinations of factor levels occur an equal number of times. For the orthogonal Latin squares L_9 it is possible to explore 4 or less design variables and their interactions using 9 points in the experimental design. In general, the maximum number of variables to be used with corresponding design is determined by the relationship: $n = (N-1)/2$, where n is the maximum number of design variables and N is the number of points in the design (9,27, or 81). See reference [13] for the explanation in detail.

2.3 Estimation of Critical Flutter Load

As shown in Figure 2, it is the time-consuming process to obtain the critical load. The response surface method with the design of experiments (DOE) is used for estimating the critical flutter load. The three-level orthogonal Latin squares is used for selecting a minimum number of points in the design space. The significance level of the factor is checked by the statistical F-test, which is genereally used for testing the similarity of two distributions. In this study, the significance level for the F-test is set to 1% and 5%.

Figure 3 shows the crtical flutter loads of the free-clamped tapered L-shaped beams subjected to a concentrated tangential follower force at the free end. The estimated critical loads are obtained by using 3-level orthogonal Latin squares $L_{27}(3^{13})$. The two design variables are the taper ratio d_1/d_0 and the slenderness ratio s_{x0}. A response surface is determined from the calculated critical flutter loads at the number of points, which are selected by the Latin squares. The estimated responses at the selected points are in good agreement with the calculated critical flutter loads .

The important generalization capability of the response surface was tested by comparing the estimated responses with the calculated critical flutter loads at any point. The error magnitudes at $d_1/d_0 = 0.875$ are 0.2% or less. In this study, the significance level for the F-test is set to 1% and 5%. In this case, the critical values are $F^{0.01} = 8.285$ and $F^{0.05} = 4.413$. When the variance ratio F_0 exceeds the critical values, the effects of each factors are considered to make the response surface function.

With increasing taper ratio d_1/d_0 and slenderness ratio s_{x0}, the critical flutter load increases monotonically.

Figure 4 shows the critical flutter loads of free-clamped tapered L-shaped beams. The 3-level orthogonal Latin squares $L_{27}(3^{13})$ is used for selecting a number of points in the design space. The two design variables are the taper ratio d_1/d_0 and the opening angle θ_1. The estimated responses at the selected points are also in good agreement with the calculated critical flutter loads. In this case, the critical values for the F-test are $F^{0.01} = 8.285$ and $F^{0.05} = 4.414$.

In order to check the generalization capability of the response surface, the critical flutter loads of beams with taper ratio $d_1 / d_0 = 0.65$ were calculated. The error magnitudes at $d_1 / d_0 = 0.65$ are 0.45% or less. With increasing taper ratio d_1 / d_0 and opening angle θ_1, the critical flutter load increases monotonically.

Figure 5 shows the crtical flutter loads of the free-clamped tapered L-shaped beams subjected to a concentrated tangential follower force at the free end. The 3-level orthogonal Latin squares $L_{27}(3^{13})$ is used for selecting a number of points in the design space. The two design variables are the slenderness ratio s_{x0} and the opening angle θ_1. The estimated responses at the selected points are also in good agreement with the calculated critical flutter loads. In this case, the critical values for the F-test are $F^{0.01} = 8.285$ and $F^{0.05} = 4.414$.

In order to check the generalization capability of the response surface, the critical flutter loads of beams with the slenderness ratio $s_{x0} = 65$ were calculated. The error magnitudes on this response surface are 0.26% or less. With increasing slenderness ratio and the opening angle, the critical flutter load increases monotonically.

Figure 6 shows the critical flutter loads of free-clamped tapered L-shaped beams. The beam has the two intermediate supports $k_1 = k_2 = 50$ at $\beta_1 = 0.05$ and β_2.The 3-level orthogonal Latin squares $L_{27}(3^{13})$ is used for selecting a number of points in the design space. The two design variables are the taper ratio d_1 / d_0 and the support position β_2. The estimated responses at the selected points are also in good agreement with the calculated critical flutter loads. In this case, the critical values for the F-test are $F^{0.01} = 8.285$ and $F^{0.05} = 4.414$.

In order to check the generalization capability of the response surface, the critical flutter loads of beams with taper ratio $d_1 / d_0 = 0.65$ were calculated. The generalization capability with an error level of 0.5% or less is excellent. With increasing taper ratio, the critical flutter load increases monotonically. When the support position β_2 moves to the free end, the critical flutter load has a maximum around $\beta_2 = 0.5$.

Figure 7 shows the crtical flutter loads of the free-clamped tapered L-shaped beams subjected to a follower force at the free end. The beam has the two intermediate supports $k_1 = k_2$ at $\beta_1 = 0.05$ and $\beta_2 = 0.5$. The 3-level orthogonal Latin squares $L_{27}(3^{13})$ is used for selecting a number of points in the design space. The two design variables are the taper ratio d_1 / d_0 and the support stiffness $k_1 = k_2$. The estimated responses at the selected points are also in good agreement with the calculated critical flutter loads. In this case, the critical values for the F-test are $F^{0.01} = 8.285$ and $F^{0.05} = 4.414$.

In order to check the generalization capability of the response surface, the critical flutter loads of beams with taper ratio $d_1 / d_0 = 0.65$ were calculated. The error

magnitudes on this response surface are 0.4% or less. With increasing taper ratio and support stiffness, the critical flutter load increases monotonically.

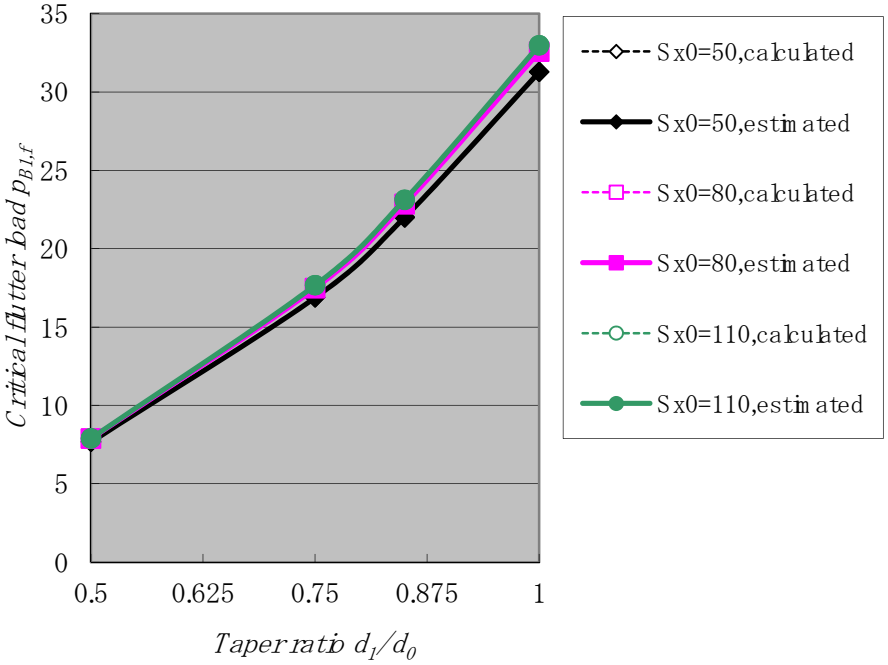

Figure 3. Critical flutter loads of L-shaped beam subjected to a concentrated follower force.

$(clamped-free, \nu = 0.3, \kappa = 0.89, \alpha_1 = 0.1, \alpha_2 = 0.1, \theta_1 = 30°, k_1 = k_2 = 0)$

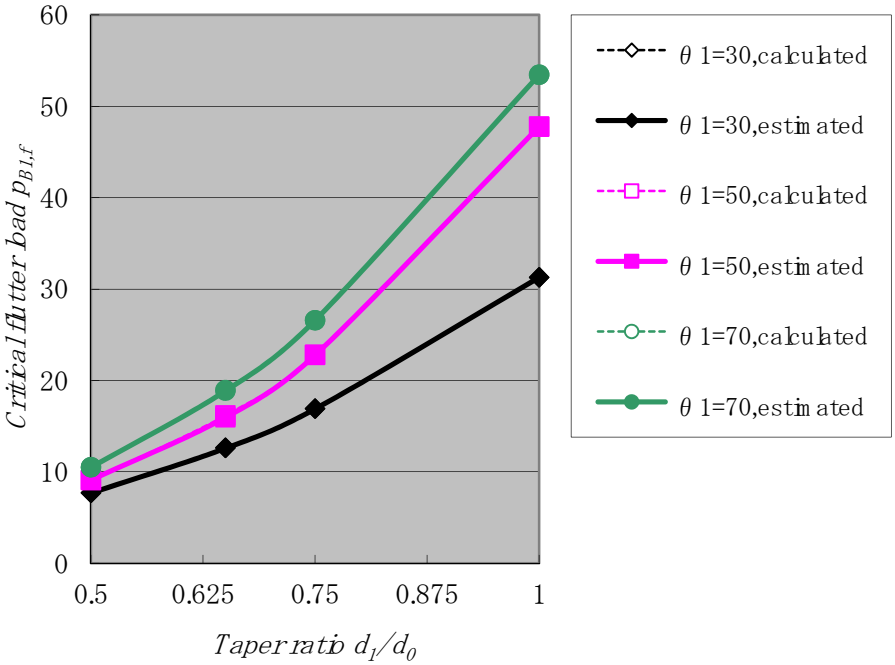

Figure 4. Critical flutter loads of L-shaped beam subjected to a concentrated follower force.

$(clamped-free, \nu = 0.3, \kappa = 0.89, \alpha_1 = 0.1, \alpha_2 = 0.1, s_{x0} = 50, k_1 = k_2 = 0)$

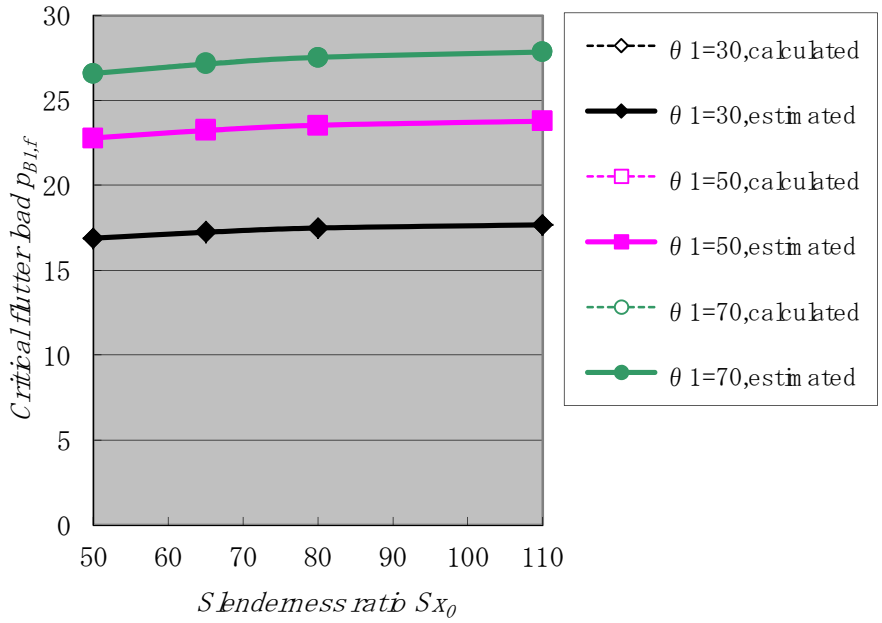

Figure 5. Critical flutter loads of L-shaped beam subjected to a concentrated follower force.
$(clamped-free, \nu=0.3, \kappa=0.89, \alpha_1=0.1, \alpha_2=0.1, d_1/d_0=0.75, k_1=k_2=0)$

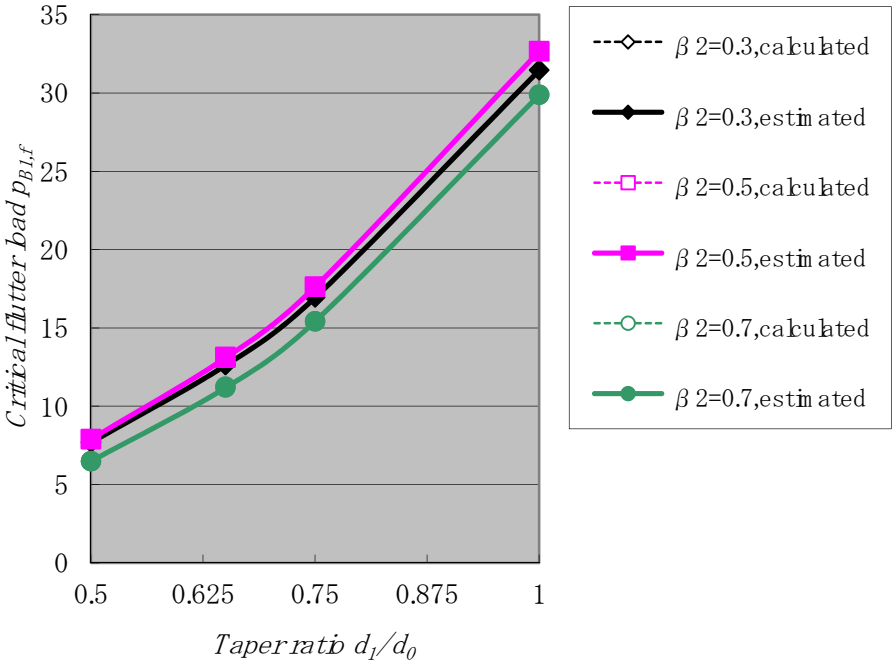

Figure 6. Critical flutter loads of L-shaped beam subjected to a concentrated follower force.
$(clamped-free, \nu=0.3, \kappa=0.89, \alpha_1=0.1, \alpha_2=0.1, s_{x0}=50, \theta_1=30°, k_1=k_2=50)$

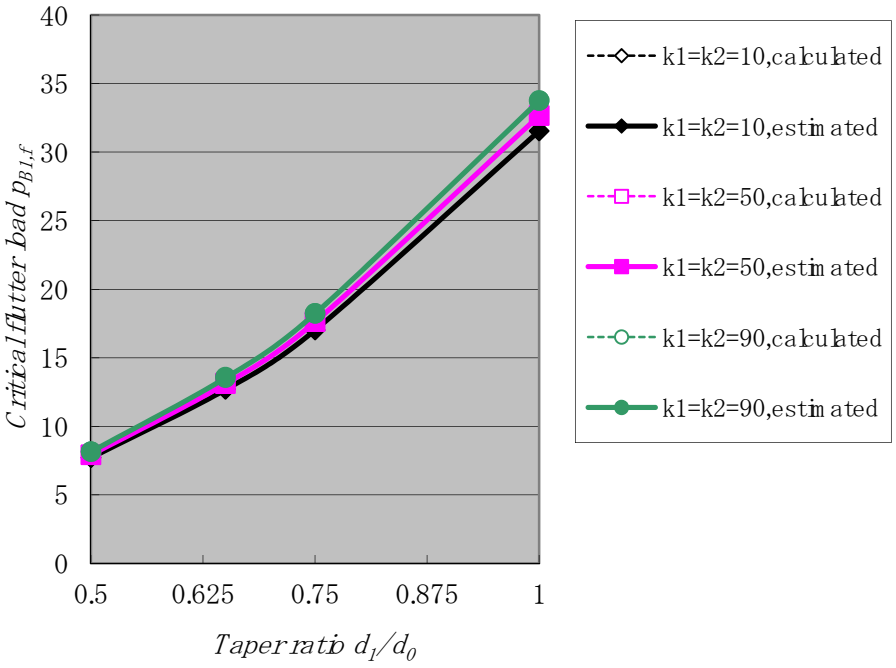

Figure 7. Critical flutter loads of L-shaped beam subjected to a concentrated follower force.
$(clamped-free, \nu=0.3, \kappa=0.89, \alpha_1=0.1, \alpha_2=0.1, s_{x0}=50, \theta_1=30°, \beta_1=0.05, \beta_2=0.5)$

3 Conclusions

In this paper the possibility of using a resopnse surface methodology, which consists of a design of experiments, for estimating the critical flutter load of the L-shaped beam was studied. Some numerical examples were presented to demonstrate the possibility of the response surface approximation. From the results of the numerical examples we can draw the following conclusions. First, the critical flutter load can be predicted by using the response surface approximation with three-level orthogonal Latin squares. Second, the generalization capability of the response surface with three-level orthogonal Latin squares $L_{27}(3^{13})$ is sufficient for estimating the critical flutter loads.

References

[1] Bolotin,V.V., " *Nonconservative Problems of Theory of Elastic Stability*", Pergamon Press, Oxford, 1963.

[2] Kounadis, A.N. and Katsikadelis, J.K., " *Shear and rotatory inertia effects on Beck's column* ", *J. Sound Vibr*. 49, 171-178,1976.

[3] Saito H. and Otomi K., "*Vibration and stability of elastically supported beams carrying an attached mass under axial and tangential loads"*, *J. Sound Vibr*. 62, 257-266, 1979.
[4] Irie T., Yamada G. and Takahashi I., "*Vibration and stability of a non-uniform Timoshenko beam subjected to a follower force", J. Sound Vibr.* 70, 503-512 ,1980.
[5] Venkateswara Rao, G. and Kanaka Raju, K. ," *Stability of tapered cantilever columns with an elastic foundation subjected to a concentrated follower force at the free end*.", *J. Sound Vibr*. 81, 147-151,1982.
[6] Lee, S.Y., Kuo, Y.H. and Lin, F.Y., " *Stability of a Timoshenko beam resting on a Winkler elastic foundation.* ", *J. Sound Vibr*. 153, 193-202,1992.
[7] Lee, S.Y. and Yang, C.C.," *Non-conservative instability of non-uniform beams resting on an elastic foundation.*", *J. Sound Vibr*. 169, 433-444,1994.
[8] De Rosa, M.A. and Franciosi, C.," *The influence of an intermediate support on the stability behavior of cantilever beams subjected to follower forces*.", *J. Sound Vibr*. 137, 107-115,1990.
[9] Takahashi, I. and Yoshioka, T. ," *Vibration and stability of a non-uniform double-beam subjected to follower forces.*", *Computers Struct*. 59, 1033-1038,1996.
[10] Singh, A., et al., "MEMS *implimentation of axial and follower end forces* ", *J. Sound Vibr,* 286, 637-644, 2005
[11] Takahashi, I. and Yoshioka, T. ," *Vibration and stability of a non-uniform L-shaped beam subjected to follower forces (in-plane vibration).*", *J.Sound Vibr*. 171, pp.255-265, 1994.
[12] Takahashi, I., "*Identification for Critical Flutter Load of a Non-uniform L-shaped Cracked Shaft subjected to a Follower Force (Out-of-Plane Vibration)*", in Topping, B.H.V., (Editor), "*Proceedings of the Seventh International Conference on the Application of Artificial Intelligence to Civil and Structural Engineering*", Civil-Comp Press, Stirlingshire, UK, Paper 58, 2003. doi:10.4203/ccp.78.58
[13] Mysers, R.H. and Montgomery, D.C.," *Response surface methodology; Process and product optimization using design experiment*", John Wiley & Sons. Inc., New York,1995.